THE JOURNAL OF PHYSICAL CHEMISTRY C
A JOURNAL OF THE AMERICAN CHEMICAL SOCIETY

pubs.acs.org/JPCC

Article

Probing the Surface Curie Temperature of Ferroelectric P(VDF-*ran*-TrFE) Copolymers by Argon Gas Cluster Ion Scattering

Mykhailo Chundak,* Claude Poleunis, Vincent Delmez, Alain M. Jonas, and Arnaud Delcorte

Cite This: *J. Phys. Chem. C* 2022, 126, 1125−1131

Read Online

ACCESS | Metrics & More | Article Recommendations | Supporting Information

ABSTRACT: This article proposes a new approach to study the temperature dependence of the structural and mechanical changes occurring at the Curie point at the surface of ferroelectric polymers. For this purpose, we used a secondary ion mass spectrometer equipped with a gas cluster ion beam. The intensities of the backscattered Ar_n^+ clusters were measured upon 10 keV Ar_{3000}^+ bombardment of a series of P(VDF-*ran*-TrFE) copolymer thin films and used to calculate the breaking ratios $Ar_2^+/(Ar_2^+ + Ar_3^+)$ and $Ar_2^+/(Ar_2^+ + Ar_4^+)$. The temperature dependences of the breaking ratios prove to be sensitive to the changes in the structural and physical properties of the polymer surfaces. The experiments reveal the transition temperature T_T (related to the bulk glass-transition temperature T_g) and the Curie temperature (T_c), indicating the ferroelectric to paraelectric transition in P(VDF-*ran*-TrFE) polymers. The results agree well with our DSC measurements and with mechanical measurements from the literature, showing that the surface Curie transition remains close to the bulk value in these copolymers. The developed approach was named gas cluster ion scattering spectrometry (GCISS), in reference to the well-known technique of ion scattering spectrometry. GCISS proves to be a versatile approach for the local measurement of structural changes occurring in polymer thin films.

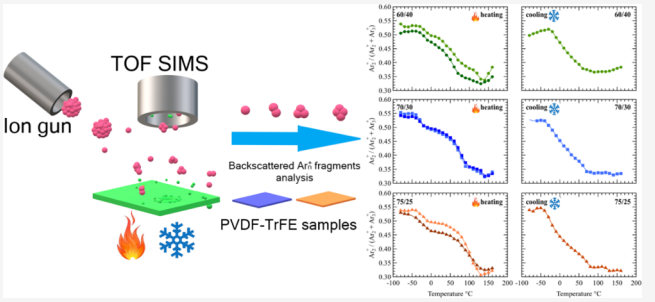

1. INTRODUCTION

Polyvinylidene fluoride−trifluoroethylene (PVDF-*ran*-TrFE) is a copolymer that is attracting attention due to its unique ferroelectric properties. It was originally developed to improve the characteristics of PVDF homopolymers, and the addition of 20−50 molar % TrFE has been shown to stabilize the copolymer in the desired ferroelectric crystalline beta phase independent of the processing method (melt or solution casting).[1] This allowed one to obtain stable ferroelectric polymer materials without the additional processing of the films with stretching.[2] P(VDF-*ran*-TrFE) is unique in the class of ferroelectric polymers because it is the first synthetic polymer in which a ferroelectric-to-paraelectric transition (Curie transition) was discovered.[3] This reversible first-order phase transition coincides with the change in the chain conformation from all-*trans* to partially *gauche* at the so-called Curie transition temperature (T_c), which occurs between room temperature and melting temperature (T_m). The change in conformation happens along with the rotational motion of the molecular chains around the chain axes and, as a result, the average dipole moment of the crystal disappears above T_c.[3] The Curie transition is a first-order transition that is characterized by a transformation between orthorhombic pseudo-hexagonal and hexagonal symmetries, causing an endothermic peak upon heating in differential scanning calorimetry (DSC), with a thermal hysteresis between heating and cooling due to the existence of nucleation barriers.[4] The exact temperature T_c varies depending on the TrFE content of the copolymer. Additionally, there are indications that heating the P(VDF-*ran*-TrFE) samples in the paraelectric phase allows the polymer chains to rearrange their orientations and positions to form a more crystalline structure upon cooling[5] and remove the residual solvent.[6] The properties of P(VDF-*ran*-TrFE) make it a desired material for a number of applications, including energy harvesting[7] and non-volatile memories.[6] Recent developments in thin-film organic electronics have renewed the interest of the scientific community in P(VDF-*ran*-TrFE) copolymers. In this context, an accurate knowledge of the Curie transition in (ultra)thin films and at interfaces is very important, as this temperature signals the upper limit of the use of the material in storage devices.

Time-of-flight secondary ion mass spectrometry (ToF SIMS) is a powerful ion beam-based technique for thin-film characterization. It provides information about the chemical, elemental, molecular, and isotopic compositions of the sample with a nanometer depth resolution and sub-micron lateral

Received: July 23, 2021
Revised: December 21, 2021
Published: January 5, 2022

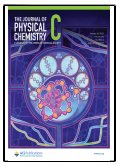

https://doi.org/10.1021/acs.jpcc.1c06564
J. Phys. Chem. C 2022, 126, 1125−1131

resolution.[8] Recently, the introduction of large gas cluster ion beams (GCIB) as projectiles has brought improvements over conventional ion beams, especially for the molecular analysis and depth profiling of organic materials.[9,10] Large gas cluster projectiles have a low kinetic energy per atom which allows them to eject molecules from organic materials with minimum damage[11] and extreme surface sensitivity.[8]

In our recent research,[12,13] we have shown that using a ToF secondary ion mass spectrometer equipped with GCIB could provide us with information about the mechanical properties of polymer thin films. In particular, polymer surface-transition temperatures (T_T), which for amorphous polymers are closely related to their glass-transition temperature (T_g), were determined[13] (T_g is the temperature at which there is sufficient free volume in the film to allow short macromolecular segments to move upon heating the polymer from the glass state[14]). For thermoset polymers, curing effects could even be followed and compared.[12] To obtain this information, a specific measurement protocol was developed, using GCIB bombardment and the ratio of backscattered argon gas cluster ions found in the positive SIMS spectra. These so-called "branching" or "breaking" ratios were first introduced by Mochiji et al.[15,16] when they noticed that the degree of dissociation of argon gas cluster ions, best illustrated by the ion intensity ratio $Ar_2^+/\Sigma Ar_n^+(n > 1)$, was correlated with the compressive stress induced upon the impact of the cluster on a series of metal surfaces. In simple words, the large gas cluster ion projectiles dissociate more extensively into small ionized clusters—which can be measured in the mass spectra—when the target is harder. Their approach was adapted by us in a protocol by which $Ar_2^+/(Ar_2^+ + Ar_3^+)$ and $Ar_2^+/(Ar_2^+ + Ar_4^+)$ breaking ratios were used to follow the change in the mechanical properties of polymer thin films. This method has certain advantages over more conventional techniques, like nanoindentation, as it avoids the interaction of an indenter with the surface and allows us to compare films with very different hardness values. In addition, ultra-thin films, down to tens of nanometers in thickness, can be measured, and complementary information like the chemical composition can be obtained from the mass spectra. In analogy to ion scattering spectrometry (ISS), we propose to coin this new variant as gas cluster ion scattering spectrometry or GCISS.

Here, the developed protocol is used for the study of the ferroelectric-to-paraelectric transition in PVDF and TrFE random copolymer P(VDF-*ran*-TrFE) thin films. This research brings additional and complementary information to the existing body of literature concerning the mechanical properties of P(VDF-*ran*-TrFE) thin films,[4,17−21] as most of the existing reports focus on their analysis from a relaxation point of view. The obtained results are compared with the DSC experiments and with data from the literature, particularly the influence of the Curie transition and high temperature on the mechanical properties of P(VDF-*ran*-TrFE). The approach demonstrated in this paper broadens the toolbox available for the polymer (ultra) thin-film characterization and opens a new avenue to explore processes occurring at their surface. The results also show that the ferro-to-paraelectric transition does not significantly differ at the surface and in the bulk of the films.

2. METHODS

2.1. Samples. For this work, three grades of P(VDF-*ran*-TrFE) random copolymers were used as provided by solvay specialty polymers. They were purchased in the form of granules and subsequently dissolved in acetyl acetone at a concentration of 35 g/L. Polymer powders were dissolved at 50 °C overnight to obtain homogeneous polymer solutions. The polymer solutions were then drop-cast on clean Si wafers (1 × 1 cm^2) covered with their native oxide layer and left for drying for 8 h at room temperature. Prior to polymer deposition, the wafers were sonicated in ethyl alcohol and dried under a N_2 flux. In the remaining of the paper, sample *X*/*Y* will denote a sample with *X* mol % of VDF and *Y* mol % of TrFE. The following samples were analyzed: 60/40, 70/30, and 75/25.

2.2. Differential Scanning Calorimetry. DSC measurements were conducted with a 821e Mettler Toledo apparatus in 40 μL aluminum pans with a N_2 flow (50 mL/min). An indium sample was used as a standard. The granule polymers of size 2−3 mm were placed in a DSC aluminum pan until 8 mg was obtained. The measurements consisted of three stages: heating, cooling, and heating again from 20 to 200 °C at a rate of 10 °C/min. The cooling and the second heating ramps are shown in Figure 1.

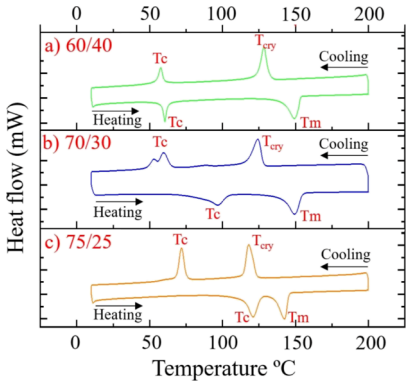

Figure 1. DSC measurements of (a) 60/40, (b) 70/30, and (c) 75/25, P(VDF-*ran*-TrFE).

2.3. ToF SIMS. ToF SIMS characterization of the samples was performed using a ToF SIMS 5 instrument (IONTOF GmbH, Münster, Germany). The apparatus is equipped with an Ar gas cluster ion beam (Ar-GCIB) mounted at 45° with respect to the sample surface. The ToF mass analyzer is perpendicular to the sample surface. The Ar-GCIB ion source was operated at 10 keV with the cluster distribution centered on Ar_{3000}^+ for both sputtering (or sputter-cleaning) and mass spectral analysis.

For spectral analyses, a raster of 128 × 128 data points over 500 × 500 μm^2 was used. The AC target current was 0.0036 pA with a bunched pulse width around 70 ns. The total dose per unit area of the primary ion beam was kept below 8×10^{11} ions/cm^2 for each analyzed region. Only positive secondary ions were analyzed. Mass resolution was $m/\Delta m \approx 280$ at 67 m/z (corresponding to $C_5H_7^+$) maintained for spectral acquisition. Sample charging was compensated with a low energy electron flood gun (E_k = 20 eV). The obtained spectra were analyzed with SurfaceLab (ver. 6.5) software that was supplied by the manufacturer. For temperature measurements, a special sample holder named "Holder G" was used, also produced by ION-TOF GmbH. The holder allows one to maintain any temperature from −150 to +600 °C through a combination of simultaneous heating and cooling, with an

https://doi.org/10.1021/acs.jpcc.1c06564
J. Phys. Chem. C 2022, 126, 1125−1131

Table 1. Characteristic Temperatures T_c (Curie Temperature), T_m (Melting Temperature), and T_{cry} (Crystallization Temperature on Cooling) of P(VDF-*ran*-TrFE) Samples as Measured by DSC and ToF SIMS Evolution of the $Ar_2^+/(Ar_2^+ + Ar_3^+)$ Breaking Ratio

	DSC (heating)		ToF SIMS °C (heating—peak values in the temperature derivative)			DSC (cooling)		ToF SIMS °C (cooling—peak values in the temperature derivative)	
composition VDF/TrFE (moles %)	T_c °C	T_m °C	T_g °C	T_c °C	T_m °C	T_c °C	T_{cry} °C	T_c °C	T_{cry} °C
60/40	~59	~150	(−17)	59	~125	~56	~128	53	113
70/30	~97	~150	(−27)	78	~130	~59	~124	61	131
75/25	~120	~144	(−23)	103	~120	~71	~118	71	124

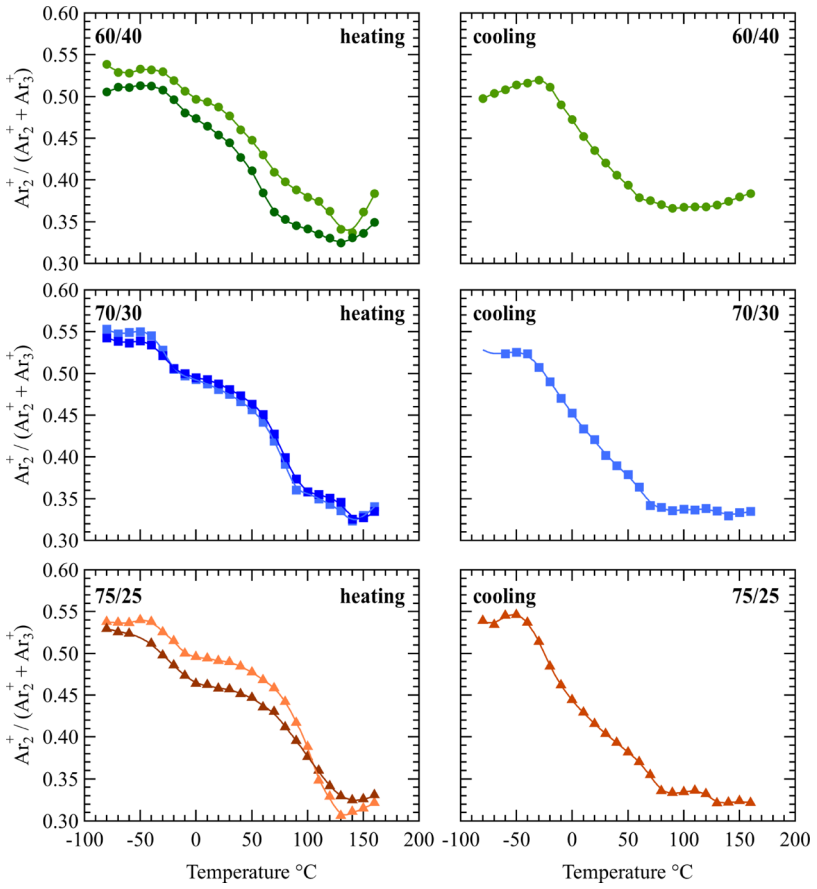

Figure 2. Evolution of the $Ar_2^+/(Ar_2^+ + Ar_3^+)$ breaking ratio as a function of temperature upon heating and cooling of P(VDF-*ran*-TrFE) thin films. The continuous lines are interpolated smoothing splines.

accuracy of ±1 °C. The temperature was stabilized for 10 min before each measurement. Before starting the actual temperature measurement series, pre-sputtering with a dose of 8×10^{14} Ar_{3000}^+/cm^2 in the DC mode was used to remove the sample surface contaminants. Afterward, continuous bombardment with a dose of 4×10^{12} Ar_{3000}^+ ions/cm^2 was performed on the same area before each measurement at a new temperature to get rid of the possible contamination occurring during temperature stabilization, as recommended in ref 13. The bombarded area was 1 × 1 mm^2.

In order to reset the thermal history of the samples, they were heated up to 160 °C and then cooled to −80 °C with the same rate. This treatment allows us to compare the SIMS measurements with the DSC measurements, upon cooling and second heating stages.

The breaking ratios reported as a function of temperature in this study correspond to the ratios of different (sum of) peak intensities, particularly $Ar_2^+/(Ar_2^+ + Ar_3^+)$ and $Ar_2^+/(Ar_2^+ + Ar_4^+)$, following the protocol presented in ref 13. They were calculated using the peak areas (counts) at the corresponding ion masses in the positive SIMS spectra of the samples. The peaks of the Ar_2^+, Ar_3^+, and Ar_4^+ ions were used because they had the highest intensities among the Ar_n^+ backscattered ions and they did not interfere with organic secondary ions emitted from the considered copolymers (Figure S1).

2.4. Thickness Measurements. The thickness of the P(VDF-*ran*-TrFE) thin films, as measured by stylus profilometry (DektakXT from Bruker Nano Surfaces Division, Tucson AZ, USA), was comprised between 1 and 6 μm depending on the copolymer formulation and the experimental batch. This thickness variation is irrelevant for SIMS analyses because the total film thickness remains orders of magnitude larger than the interaction depth of the 10 keV Ar_{3000}^+ ions used to probe the film surfaces.

https://doi.org/10.1021/acs.jpcc.1c06564
J. Phys. Chem. C 2022, 126, 1125−1131

3. RESULTS AND DISCUSSION

3.1. DSC Measurements. The successive DSC curves of the samples are presented in Figure 1 with their characteristic temperatures collected in Table 1. The heating ramps feature two endothermic peaks with the first one being T_c, associated with the ferro-to-paraelectric transition at the Curie temperature, and the second one being T_m, corresponding to the melting of the paraelectric crystalline phase. For the 60/40 sample, T_c was found at ∼59 °C and T_m at ∼150 °C. With the increase of the mol % of VDF in the samples, the T_c shifts to higher temperatures while T_m varies very little.

The cooling DSC ramps in Figure 1 feature two exothermic peaks for each P(VDF-*ran*-TrFE) sample. The peaks at higher temperatures correspond to the crystallization of the films (T_{cry}) while the peaks at lower temperatures are attributed to the Curie transition temperature T_c, as shown in Table 1. In the case of the 70/30 sample, the Curie transition peak is bimodal and usually ascribed to the para-ferroelectric transition with the formation of perfect and defective structures.[21]

3.2. Ar Cluster Backscattering Measurements. For the sake of conciseness only the evolution of the $Ar_2^+/(Ar_2^+ + Ar_3^+)$ breaking ratio is shown here as a function of heating and cooling of the copolymers 60/40, 70/30, and 75/25, as shown in Figure 2. The $Ar_2^+/(Ar_2^+ + Ar_4^+)$ breaking ratio is shown in Figure S2. All the samples were measured from (−80 to 160 °C) and cooled back to (−80) °C. This temperature range should allow us to measure the phase transitions including surface T_g (T_T), T_c, T_m, or T_{cry} as discussed below. The heating plots (−80 to 160 °C) include two measurements conducted on different samples and days, showing the repeatability of the experiments.

All the heating curves of P(VDF-*ran*-TrFE) samples show similar features, quite different from those observed on simpler thermoplastic[13] and thermoset polymers.[12] The curves exhibit a low-temperature plateau, with the highest breaking ratio values (between 0.50 and 0.55) before undergoing the first descending slope over [(−40) to (−10) °C], which can be attributed to the surface glass transition of the polymer. The temperature range of this first decrease agrees well with the bulk value of T_g found by Teyssedre et al. for a 75/25 sample (T_g ∼ (−36) °C).[22] The glass transition ends by a (semi-)plateau followed by a region of faster decrease, over an extended range of temperatures which depends on the copolymer formulation. This region ends with a third (semi-) plateau, which is followed for samples 60/40 and 70/30 by a change of the sign of the temperature slope. The $Ar_2^+/(Ar_2^+ + Ar_4^+)$ curves indicate essentially the same temperature regions (Figure S2). The lowest $Ar_2^+/(Ar_2^+ + Ar_3^+)$ value is close to 0.3 [0.7 for $Ar_2^+/(Ar_2^+ + Ar_4^+)$], remaining slightly higher than for thermoplastic polymers and thermosets with a low degree of curing.

In order to have a more accurate view of the thermal evolution of the breaking ratios, the experimental curves were interpolated by a smoothing spline procedure (continuous lines in Figure 2) and their temperature derivatives were computed (Figure 3a). In these curves, a broad negative peak corresponding to the surface glass transition (T_T) appears between (−40) and (−10) °C (vertical dashed lines in Figure 3a), essentially independent of the copolymer composition. It is followed by a second negative peak shifting toward higher temperatures for higher VDF contents (arrows in Figure 3a), whose temperature location correlates well with the Curie

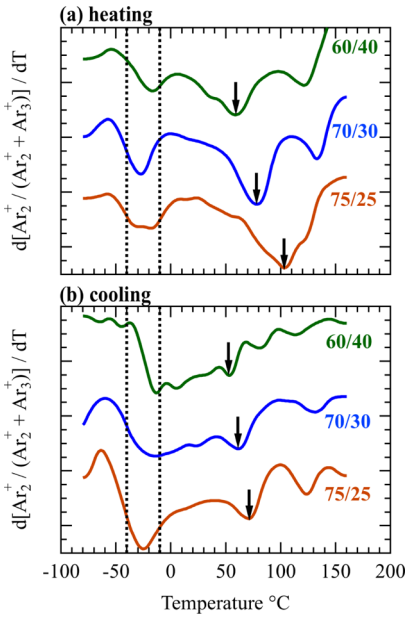

Figure 3. Temperature derivatives of the $Ar_2^+/(Ar_2^+ + Ar_3^+)$ breaking ratios as a function of temperature upon heating and cooling of P(VDF-*ran*-TrFE) thin films of different VDF/TrFE contents (as indicated). For the heating curves, the average derivatives of the two experiments were computed. The vertical dashed lines indicate the glass−transition temperature and arrows signal the ferro-to-paraelectric Curie transition. The derivatives are shifted vertically for clarity.

transition measured by DSC (Figure 4), confirming that the second rapid decrease of the breaking ratio results from the

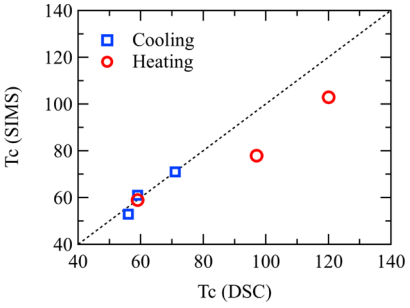

Figure 4. Correlation between the ferro-to-paraelectric (Curie) transition temperatures as measured by ToF SIMS (arrows in Figure 3) and by DSC on heating (red circles) and on cooling (blue squares). The dashed line is the equivalence line of 45° slope.

ferro-to-paraelectric transition. A third higher temperature negative peak then appears at 120−130 °C for samples 60/40 and 70/30; this peak only appears as a shoulder for sample 75/25 (Figure 3a). This third peak broadly correlates to the onset of melting of the samples in the DSC traces. In this respect, it is important to remember that melting is a progressive process in polymers, due to the distribution of crystal thickness and perfection, resulting in a considerable broadening of the transition.

The cooling curves of the breaking ratio display less clear-cut features (Figure 2), and their temperature derivatives (Figure 3b) are generally more noisy. Nevertheless, the derivatives still show a higher temperature negative peak falling in the same range as the DSC crystallization exotherm (T_{cry}), an

https://doi.org/10.1021/acs.jpcc.1c06564
J. Phys. Chem. C 2022, 126, 1125−1131

intermediate negative peak (arrows in Figure 3b) whose location correlates with the Curie temperature measured on cooling by DSC (Figure 4), and a strong perturbation in the glass transition range (vertical dashed lines in Figure 3b).

3.3. Discussion. The good correlation between the transition temperatures measured by DSC and SIMS provides a strong support to the identification of the Curie transition in the temperature dependence of the SIMS breaking ratio. In previous works, the value of the breaking ratios was shown to be influenced primarily by the mechanical properties of the surface (hardness or resistance to deformation, elastic modulus).[12,13] The ToF SIMS results can be compared to the microindentation hardness measurements performed on P(VDF-*ran*-TrFE) samples by Balta Calleja et al.[18] and to the measurements of the remanent polarization and Young's modulus in ref 23, even though the experiments were conducted in a different temperature range with a different annealing speed. In ref 16, the authors showed a dramatic decrease of hardness occurring at the onset of the Curie transition, with an important change of the temperature dependence of the hardness from that point on. The similarity of the temperature-dependent hardness curves obtained by these authors with the temperature dependence of the breaking ratios measured in the present work is striking, in the temperature range of the ferro-to-paraelectric transition. This similarity, together with the good agreement between the transition temperatures obtained by DSC and SIMS, confirms the sensitivity of ToF SIMS measurements to the changes of mechanical properties; while this was already demonstrated for the glass transition, our current work significantly extends this demonstration to a first-order Curie transition.

Additionally, the glass transition region generally reproduces our previous findings.[12] However, it is less easy to distinguish it on cooling, which probably results from the proximity of the Curie temperature. A more complex behavior is observed in the melting and crystallization ranges, which requires a more detailed discussion. The increase in the values of the breaking ratios above 120−130 °C is especially intriguing. In our previous research we showed that the linear increase of the Ar_n^+ ion intensities with temperature was canceled out in the breaking ratios, thus other factors should influence the observed increase. The extensive surface cleaning by Ar cluster pre-sputtering before thermal cycling also allows us to exclude the influence of contaminants, so we can safely assume that it is caused by the crystalline structure or morphological change of the polymeric layer. On the other hand, the microscopic pictures of the coatings as a function of temperature (Figure S3) suggesting that there could be some de-wetting of the polymeric film occurring in the melt, which could expose a fraction of the bare silicon surface to the beam. The gradual exposure of the much harder Si substrate could explain a slow increase of the breaking ratio beyond T_m.

For the 60/40 sample, an additional measurement cycle was conducted but with a maximum temperature of 110 °C, that is, reasonably below the expected T_m (Figure S4). The breaking ratio $Ar_2^+/(Ar_2^+ + Ar_3^+)$ follows a very similar path upon cooling than that of the sample heated up to 160 °C, suggesting that the processes happening above T_m are reversible. The derivatives of the curves obtained for both 60/40 samples, heated to 160 and 110 °C, respectively, are shown in Figure S5. The data demonstrate a good agreement between the two experiments, except for a slight shift of the measured Curie temperature (as one would expect). A set of measurements was also conducted without resetting the thermal history by annealing and even though the curves show some unexplained differences, they indicate similar Curie temperatures (see the case of the 70/30 sample in Figure S6).

The data of gradual heating and cooling of the polymers suggest a similar general behavior but with clearly distinct characteristic temperatures as a function of the composition. According to our interpretation and in agreement with DSC measurements, the polymers have individual T_g, T_c ranges, and paraelectric region ending with T_m. The main difference among the samples is the Curie transition range which moves to higher temperatures with increasing VDF content in the samples. As quantitatively shown in Table 1, the ToF SIMS-determined thermal transitions for each sample are near the temperatures obtained by DSC, supporting our description of the transformations occurring in the films based on the breaking ratio curves. However, the two measurements provide different and complementary information. While the DSC measurements show the change of heat capacity accompanying the glass transition, and the heat flow due to structural transformations, the evolution of the breaking ratios reflects the associated change in the mechanical properties of the films, as in Balta Calleja et al.[18] This agrees with the results of our previous work where we showed that the temperature dependences of the breaking ratios were reminiscent of dynamic mechanical and torsional braid measurements. Thus, we can conclude that this protocol gives us a new method to follow the ferroelectric to paraelectric transformation in the P(VDF-*ran*-TrFE) thin films, simultaneously with the measurement of the chemical composition of the films. More generally, it opens new research possibilities for other organic thin films undergoing structural/phase transitions with temperature or other external factors. At this stage of research, our measurements remain largely qualitative. However, a detailed comparison with other characterization methods (e.g., AFM) and modeling of the cluster impact and fragmentation give us hope that more quantitative measurements utilizing Ar cluster breaking ratios will be attained.

As a final note, a recent study showed that 70/30 mol % P(VDF-*ran*-TrFE) film surfaces are formed of ∼100 nm rice-like crystalline domains intermixed with amorphous regions.[24] Local measurements indicate large variations of the modulus not only between the grains and the surrounding medium but also within the grains, when going from crystalline lamellae to amorphous layers. At the Curie transition, the morphology evolves from a densely packed assembly of crystalline grains to a more loose arrangement where the properties are dominated by the amorphous phase surrounding the crystals. In comparison, the interaction of the 10 keV Ar_{3000}^+ clusters is intrinsically nanoscale because the clusters themselves are a few nm in size, and the craters created in polymers exhibit a diameter of 10−20 nm maximum according to MD simulations,[25] with the molecular emission from the top nanometer. However, the ion beam scans a square area of a few hundreds of micrometer in lateral dimensions, meaning that the backscattered ion signals are averaged over this area and the local information is lost. If event-by-event (i.e., separate impact) counting[26] was possible with our instrument and bombardment conditions, it might also reveal bi- (or multi)modal distributions of breaking ratios, depending on the exact impact locations of the clusters on the surface.

https://doi.org/10.1021/acs.jpcc.1c06564
J. Phys. Chem. C 2022, 126, 1125−1131

4. CONCLUSIONS

In addition to MS and soft desorption of polymeric samples, GCIB provide information on the surface physical and structural changes via the backscattering of small argon cluster ions. In this research, the backscattered Ar_n^+ (n = 2, 3, 4) clusters were used to study the ferroelectric to paraelectric transitions in P(VDF-*ran*-TrFE) polymers. The surface of P(VDF-*ran*-TrFE) thin films was bombarded by 10 keV Ar_{3000}^+ clusters, and the intensity of the resultant backscattered ionized fragments Ar_n^+ (n = 1, 2, 3, 4) was measured with our ToF mass spectrometer. The temperature dependence of the intensity (breaking) ratios $Ar_2^+/(Ar_2^+ + Ar_3^+)$ and $Ar_2^+/(Ar_2^+ + Ar_4^+)$ was measured between (−80) and +160 °C for 60/40, 70/30, and 75/25 P(VDF-*ran*-TrFE) formulations. The characteristic curves, with their distinctive patterns, follow the changes in the mechanical properties of the films, in line with microindentation measurements, and indicate the specific values of the surface Curie temperatures (T_c) of the three samples, which are remarkably close to those measured by DSC. This is an important result of the study, showing that the ferro-to-paraelectric transition does not significantly differ at the surface and in the bulk.

The obtained data also allow us to conclude that backscattered Ar_n^+ clusters can be used for the investigation of the temperature regions of ferroelectric to paraelectric transitions occurring at the surface of P(VDF-*ran*-TrFE) copolymers. More importantly, this new study demonstrates once again the efficacy and robustness of GCISS for the measurement of surface transition temperatures, including a Curie transition. In particular, it shows the sensitivity of the method to more subtle changes of the structure and mechanical properties than those happening at the glass-transition temperature. Though the link between the breaking ratios and the mechanical properties of the polymer, such as Young's modulus and hardness, remains qualitative at this stage, GCISS inherently possesses the μm lateral resolution and the nm depth resolution permitted by the ion beam focus and the physics of the cluster−surface interaction. Two-dimensional mappings and even three-dimensional reconstructions of the data could then prove to be very useful in the case of the structured organic samples and multilayers.

■ ASSOCIATED CONTENT

Supporting Information

The Supporting Information is available free of charge at https://pubs.acs.org/doi/10.1021/acs.jpcc.1c06564.

ToF SIMS spectra of P(VDF-*ran*-TrFE) 60/40, 70/30, and 75/25; evolution of the $Ar_2^+/(Ar_2^+ + Ar_4^+)$ breaking ratios as a function of temperature upon heating and cooling of P(VDF-*ran*-TrFE) thin films 60/40, 70/30, and 75/25; microscopic pictures of the coatings of the P(VDF-*ran*-TrFE) 75/25 sample; evolution of the $Ar_2^+/(Ar_2^+ + Ar_3^+)$ and $Ar_2^+/(Ar_2^+ + Ar_4^+)$ breaking ratios as a function of temperature upon heating to 110 °C and cooling of the P(VDF-*ran*-TrFE) 60/40 sample; temperature derivative of the $Ar_2^+/(Ar_2^+ + Ar_3^+)$ breaking ratio of the P(VDF-*ran*-TrFE) 60/40 sample as a function of temperature upon heating; temperature derivative of the $Ar_2^+/(Ar_2^+ + Ar_3^+)$ breaking ratio of the P(VDF-*ran*-TrFE) 70/30 sample; evolution of the $Ar_2^+/(Ar_2^+ + Ar_4^+)$ breaking ratio as a function of temperature upon heating P(VDF-*ran*-TrFE) thin films 60/40, 70/30, and 75/25; and their respective temperature derivatives of the $Ar_2^+/(Ar_2^+ + Ar_4^+)$ ratio (PDF)

■ AUTHOR INFORMATION

Corresponding Author

Mykhailo Chundak − *Institute of Condensed Matter and Nanosciences (IMCN), Université catholique de Louvain (UCL), Louvain-la-Neuve B-1348, Belgium;* orcid.org/0000-0003-4417-1832; Email: Arnaud.delcorte@uclouvain.be

Authors

Claude Poleunis − *Institute of Condensed Matter and Nanosciences (IMCN), Université catholique de Louvain (UCL), Louvain-la-Neuve B-1348, Belgium*

Vincent Delmez − *Institute of Condensed Matter and Nanosciences (IMCN), Université catholique de Louvain (UCL), Louvain-la-Neuve B-1348, Belgium;* orcid.org/0000-0002-9203-9919

Alain M. Jonas − *Institute of Condensed Matter and Nanosciences (IMCN), Université catholique de Louvain (UCL), Louvain-la-Neuve B-1348, Belgium;* orcid.org/0000-0002-4083-0688

Arnaud Delcorte − *Institute of Condensed Matter and Nanosciences (IMCN), Université catholique de Louvain (UCL), Louvain-la-Neuve B-1348, Belgium;* orcid.org/0000-0003-4127-8650

Complete contact information is available at: https://pubs.acs.org/10.1021/acs.jpcc.1c06564

Notes

The authors declare no competing financial interest.

■ ACKNOWLEDGMENTS

The authors wish to thank T. Daphnis for performing the P(VDF-*ran*-TrFE) film thickness measurements. M.C. would like to acknowledge the "Fonds National de la Recherche Scientifique" (FNRS) for financing the project CLUSTERPROBE under the convention PDR T.0065.18. V.D. acknowledges the financial support of the Fédération Wallonie Bruxelles, through the project "iBEAM" funded by its research program "Actions de Recherche Concertées" (Convention n°18/23-090). A.D. is a Research Director of FNRS.

■ REFERENCES

(1) Martins, P.; Lopes, A. C.; Lanceros-Mendez, S. Electroactive Phases of Poly(Vinylidene Fluoride): Determination, Processing and Applications. *Prog. Polym. Sci.* **2014**, *39*, 683−706.

(2) Sencadas, V.; Gregorio, R.; Lanceros-Méndez, S. α to β Phase Transformation and Microestructural Changes of PVDF Films Induced by Uniaxial Stretch. *J. Macromol. Sci., Part B* **2009**, *48*, 514−525.

(3) Tanaka, R.; Tashiro, K.; Kobayashi, M. Annealing Effect on the Ferroelectric Phase Transition Behavior and Domain Structure of Vinylidene Fluoride (Vdf)−Trifluoroethylene Copolymers: A Comparison between Uniaxially Oriented Vdf 73 and 65% Copolymers. *Polymer* **1999**, *40*, 3855−3865.

(4) Bargain, F.; Thuau, D.; Panine, P.; Hadziioannou, G.; Domingues Dos Santos, F.; Tencé-Girault, S. Thermal Behavior of Poly(Vdf-Ter-Trfe-Ter-Ctfe) Copolymers: Influence of Ctfe Termonomer on the Crystal-Crystal Transitions. *Polymer* **2019**, *161*, 64−77.

(5) Furukawa, T.; Nakajima, T.; Takahashi, Y. Factors Governing Ferroelectric Switching Characteristics of Thin Vdf/Trfe Copolymer Films. *IEEE Trans. Dielectr. Electr. Insul.* **2006**, *13*, 1120−1131.

(6) Mao, D.; Quevedo-Lopez, M. A.; Stiegler, H.; Gnade, B. E.; Alshareef, H. N. Optimization of Poly(Vinylidene Fluoride-Trifluoroethylene) Films as Non-Volatile Memory for Flexible Electronics. *Org. Electron.* **2010**, *11*, 925−932.
(7) Nunes-Pereira, J.; Sencadas, V.; Correia, V.; Rocha, J. G.; Lanceros-Méndez, S. Energy Harvesting Performance of Piezoelectric Electrospun Polymer Fibers and Polymer/Ceramic Composites. *Sens. Actuators, A* **2013**, *196*, 55−62.
(8) Vickerman, J. C.; Briggs, D. *Tof-Sims Materials Analysis by Mass Spectrometry*, 2nd ed.; IM Publications and SurfaceSpectra Limited: Manchester, 2013.
(9) Ninomiya, S.; Ichiki, K.; Nakata, Y.; Honda, Y.; Seki, T.; Aoki, T.; Matsuo, J. Secondary Ion Emission from Si Bombarded with Large Ar Cluster Ions under Uhv Conditions. *Appl. Surf. Sci.* **2008**, *255*, 880−882.
(10) Delcorte, A.; Delmez, V.; Dupont-Gillain, C.; Lauzin, C.; Jefford, H.; Chundak, M.; Poleunis, C.; Moshkunov, K. Large Cluster Ions: Soft Local Probes and Tools for Organic and Bio Surfaces. *Phys. Chem. Chem. Phys.* **2020**, *22*, 17427−17447.
(11) Delcorte, A.; Cristaudo, V.; Lebec, V.; Czerwinski, B. Sputtering of Polymers by Kev Clusters: Microscopic Views of the Molecular Dynamics. *Int. J. Mass Spectrom.* **2014**, *370*, 29−38.
(12) Chundak, M.; Poleunis, C.; Delmez, V.; Jefford, H.; Bonnaud, L.; Jonas, A. M.; Delcorte, A. Argon Gas Cluster Fragmentation and Scattering as a Probe of the Surface Physics of Thermoset Polymers. *Appl. Surf. Sci.* **2020**, *533*, 147473.
(13) Poleunis, C.; Cristaudo, V.; Delcorte, A. Temperature Dependence of Arn+ Cluster Backscattering from Polymer Surfaces: A New Method to Determine the Surface Glass Transition Temperature. *J. Am. Soc. Mass Spectrom.* **2018**, *29*, 4−7.
(14) Painter, P. C.; Coleman, M. M. *Fundamentals of Polymer Science an Introductory Text*; Technomic Publishing Company, Inc.: Lancaster, US, 1994.
(15) Mochiji, K.; Se, N.; Inui, N.; Moritani, K. Mass Spectrometric Analysis of the Dissociation of Argon Cluster Ions in Collision with Several Kinds of Metal. *Rapid Commun. Mass Spectrom.* **2014**, *28*, 2141−2146.
(16) Inui, N.; Mochiji, K.; Moritani, K. A Nondestructive Method for Probing Mechanical Properties of a Thin Film Using Impacts with Nanoclusters. *Int. J. Appl. Mech.* **2016**, *08*, 1650041.
(17) Ngoma, J. B.; Cavaille, J. Y.; Paletto, J.; Perez, J. Curie Transition Study in a 7030mol% Copolymer of Vinylidene Fluoride and Trifluoroethylene by Mechanical Spectrometry. *Polymer* **1991**, *32*, 1044−1048.
(18) Baltá Calleja, F. J.; Santa Cruz, C.; González Arche, A.; López Cabarcos, E. Temperature Dependence of Microhardness and Structure of Ferroelectric Copolymers of Vinylidene Fluoride. *J. Mater. Sci.* **1992**, *27*, 2124−2130.
(19) Omote, K.; Ohigashi, H.; Koga, K. Temperature Dependence of Elastic, Dielectric, and Piezoelectric Properties of "Single Crystalline" Films of Vinylidene Fluoride Trifluoroethylene Copolymer. *J. Appl. Phys.* **1997**, *81*, 2760−2769.
(20) Mano, J. F.; Sencadas, V.; Costa, A. M.; Lanceros-Méndez, S. Dynamic Mechanical Analysis and Creep Behaviour of B-Pvdf Films. *Mater. Sci. Eng. A* **2004**, *370*, 336−340.
(21) Roggero, A.; Dantras, E.; Lacabanne, C. Poling Influence on the Mechanical Properties and Molecular Mobility of Highly Piezoelectric P(Vdf-Trfe) Copolymer. *J. Polym. Sci., Part B: Polym. Phys.* **2017**, *55*, 1414−1422.
(22) Teyssedre, G.; Bernes, A.; Lacabanne, C. Dsc and Tsc Study of a Vdf/Trfe Copolymer. *Thermochim. Acta* **1993**, *226*, 65−75.
(23) Hafner, J.; Teuschel, M.; Schneider, M.; Schmid, U. Origin of the Strong Temperature Effect on the Piezoelectric Response of the Ferroelectric (Co-)Polymer P(Vdf70-Trfe30). *Polymer* **2019**, *170*, 1−6.
(24) Hafner, J.; Benaglia, S.; Richheimer, F.; Teuschel, M.; Maier, F. J.; Werner, A.; Wood, S.; Platz, D.; Schneider, M.; Hradil, K.; et al. Multi-Scale Characterisation of a Ferroelectric Polymer Reveals the Emergence of a Morphological Phase Transition Driven by Temperature. *Nat. Commun.* **2021**, *12*, 152.
(25) Delcorte, A.; Moshkunov, K.; Debongnie, M. Relationships between Crater and Sputtered Material Characteristics in Large Gas Cluster Sputtering of Polymers: Results from Molecular Dynamics Simulations. *J. Vac. Sci. Technol., B* **2018**, *36*, 03F109.
(26) Eller, M. J.; Chandra, K.; Coughlin, E. E.; Odom, T. W.; Schweikert, E. A. Label Free Particle-by-Particle Quantification of DNA Loading on Sorted Gold Nanostars. *Anal. Chem.* **2019**, *91*, 5566−5572.

https://doi.org/10.1021/acs.jpcc.1c06564
J. Phys. Chem. C 2022, 126, 1125−1131